Cancer Immunotherapy

International Edition: DOI: 10.1002/anie.201500799
German Edition: DOI: 10.1002/ange.201500799

Multiformat T-Cell-Engaging Bispecific Antibodies Targeting Human Breast Cancers**

Yu Cao, Jun Y. Axup, Jennifer S. Y. Ma, Rongsheng E. Wang, Seihyun Choi, Virginie Tardif, Reyna K. V. Lim, Holly M. Pugh, Brian R. Lawson, Gus Welzel, Stephanie A. Kazane, Ying Sun, Feng Tian, Shailaja Srinagesh, Tsotne Javahishvili, Peter G. Schultz, and Chan Hyuk Kim**

Abstract: *Four different formats of bispecific antibodies (bsAbs) were generated that consist of anti-Her2 IgG or Fab site-specifically conjugated to anti-CD3 Fab using the genetically encoded noncanonical amino acid. These bsAbs varied in valency or in the presence or absence of an Fc domain. Different valencies did not significantly affect antitumor efficacy, whereas the presence of an Fc domain enhanced cytotoxic activity, but triggered antigen-independent T-cell activation. We show that the bsAbs can efficiently redirect T cells to kill all Her2 expressing cancer cells, including Her2 1+ cancers, both in vitro and in rodent xenograft models. This work increases our understanding of the structural features that affect bsAb activity, and underscores the potential of bsAbs as a promising therapeutic option for breast cancer patients with low or heterogeneous Her2 expression.*

Human epidermal growth factor receptor 2 (Her2) specific monoclonal antibodies, including trastuzumab and pertuzumab, and the recently approved antibody drug conjugate (ADC), trastuzumab emtansine (T-DM1), have markedly improved the prognosis for Her2-positive cancer patients.[1–3] However, a retrospective subgroup analysis of the clinical trials suggests that these agents are most effective in patients with Her2 overexpressing breast cancers (scored 3+ or 2+ by immunohistochemistry, IHC, and confirmed by fluorescence in situ hybridization, FISH), leaving a significant unmet medical need for patients with tumors that have low levels of Her2 expression (scored 1+, ≈30% of breast cancer patients).[4,5] Recently, T-cell-recruiting bispecific antibodies (bsAbs) that simultaneously bind tumor-associated antigens and an invariant component of the T-cell receptor (e.g., CD3 epsilon), have shown excellent clinical efficacy in the treatment of hematological malignances and various solid tumors.[6] Because the activation of T cells by bsAbs does not rely on high copy numbers of the surface tumor antigen nor its intracellular trafficking,[7,8] bsAbs may provide enhanced efficacy for cancer cells that express low levels of Her2, relative to ADC. Indeed, potent efficacy of Her2-targeted bsAbs has been previously demonstrated against tumor cells with low Her2 expression.[8,9] Moreover, due to multiple cytotoxic mechanisms, T cells engaged by bsAbs can potently target chemotherapy-resistant cancer cells and quiescent cancer stem cells.[10–12] However, to prevent severe side effects, such as cytokine release syndrome (CRS),[13] antigen-independent T-cell activation by bsAbs must be minimized.

Most current methods for the generation of bsAbs rely on genetic methods, such as the fusion of engineered antibody fragments (e.g., BiTE, DART, and Diabody) or the heterodimeric pairing of heavy chains (e.g., Triomab and CrossMab).[14,15] Previously, we reported a general method to synthesize bsAbs by genetically incorporating the noncanonical amino acid *p*-acetylphenylalanine (pAcF) into the Fab fragments of antibodies.[16] This method allows for conjugation of two distinct antibodies with control over the sites of conjugation and linker length in order to optimize immunological synapse formation. Herein, we further explore this approach by synthesizing several structurally distinct bsAbs and determining how variations in structure affect activity. BsAbs were constructed that bind Her2 and CD3 in either monovalent or bivalent mode, and either with or without a functional Fc domain. We examined the effects of valency and the presence of an Fc domain on the in vitro cytotoxicity, pharmacokinetics, off-target toxicity, and in vivo efficacy of these bsAbs using human breast tumors expressing different levels of Her2, and also compared the activity of these bsAbs to an anti-Her2 ADC consisting of trastuzumab conjugated with monomethyl auristatin F (T-nAF).

To vary valency and Fc receptor engagement by the bsAbs, we site-specifically incorporated pAcF into the anti-Her2 antibody trastuzumab, and the anti-CD3 antibody UCHT1 at one [anti-Her2 IgG (HA121X), anti-Her2 Fab (LS202X), and anti-CD3 Fab (HK138X)] or two [anti-CD3 Fab (LS202X/HK138X)] distinct sites (where X designates pAcF). All of the pAcF sites are located in constant regions of

[*] Dr. Y. Cao,[+] Dr. J. Y. Axup,[+] Dr. R. E. Wang, Dr. S. Choi, Prof. P. G. Schultz
Department of Chemistry and The Skaggs Institute for Chemical Biology, The Scripps Research Institute
10550 N Torrey Pines Rd, La Jolla, CA 92037 (USA)
E-mail: Schultz@scripps.edu
Dr. V. Tardif, Dr. B. R. Lawson
Department of Immunology and Microbial Science
The Scripps Research Institute (USA)
Dr. J. S. Y. Ma, Dr. R. K. V. Lim, H. M. Pugh, G. Welzel, Dr. S. A. Kazane, Prof. P. G. Schultz, Dr. C. H. Kim
California Institute for Biomedical Research
11119 N Torrey Pines Rd, La Jolla, CA 92037 (USA)
E-mail: chkim@calibr.org
Dr. Y. Sun, Dr. F. Tian, S. Srinagesh, Dr. T. Javahishvili
EuCode Technology, Ambrx, Inc.
10975 N Torrey Pines Rd, La Jolla, CA 92037 (USA)
[+] These authors contributed equally to this work.
[**] This work was supported by NIH grant 5R01 GM062159-13 (P.G.S.).
Supporting information for this article is available on the WWW under http://dx.doi.org/10.1002/anie.201500799.

the antibodies, and were previously used for various site-specific modifications without affecting the binding affinity of the molecules.[17,18] The mutant Fabs were expressed in *Escherichia coli* (*E. coli*)[19] using an orthogonal *M. jannaschii*-derived tRNA/aminoacyl-tRNA synthetase ($tRNA_{CUA}$/pAcFRS) pair that selectively incorporates pAcF into proteins in response to UAG with typical yields of 3–5 $mg\,L^{-1}$. The IgG with pAcF was expressed in suspension CHO cells ($\approx 10\,mg\,L^{-1}$ yield from transient transfection) with an *E. coli*-derived $tRNA_{CUA}$/pAcFRS pair.[20] Next, the keto group of the mutant antibodies was site-specifically modified by forming an oxime linkage with bifunctional polyethylene glycol linkers containing an alkoxyamine on one terminus and an azide (anti-Her2 antibody) or cyclooctyne (anti-CD3 antibody) group on the other terminus (Figure S1 in the Supporting Information, SI). The conjugation efficiency (>90%) was verified by ESI-MS (Table S1). This approach allows to couple the full length IgGs and Fabs in various formats using a copper-free [3+2] Huisgen cycloaddition reaction ("Click" reaction).[21,22]

As shown in Figure 1A, we designed four different IgG- and Fab-based bsAbs that bind Her2 and CD3 in either a monovalent or bivalent mode: Tetra-IgG (bivalent Her2 and CD3 binding), Tri-IgG (bivalent Her2 and monovalent CD3 binding), TriFab (bivalent Her2 and monovalent CD3 binding), and BiFab (monovalent Her2 and CD3 binding). In addition, the IgG-based bsAbs (Tetra-IgG and Tri-IgG) contain a functional Fc domain, which may affect the overall efficacy and selectivity of the constructs. Each bsAb was synthesized by coupling the corresponding linker-modified antibodies at the appropriate concentration using a copper-free Click reaction. Since IgG is homodimeric, the modified anti-Her2 IgG (HA121X) has two reaction sites per molecule, and its reaction with excess anti-CD3 Fab (HK138X) yields Tetra-IgG. On the other hand, a 1:1 molar ratio of the linker-modified anti-Her2 IgG (HA121X) and anti-CD3 Fab (LS202X/HK138X) leads predominantly to the formation of Tri-IgG. TriFab was synthesized from the reaction of modified anti-CD3 Fab (LS202X/HK138X) with excess anti-Her2 Fab (LS202X). Lastly, BiFab was prepared by incubating an equal molar ratio of modified anti-Her2 Fab (LS202X) and anti-CD3 Fab (HK138X; SI). Following conjugation and purification by size exclusion chromatography, the final yield was 50% for Tetra-IgG, 25% for Tri-IgG, 30% for TriFab, and 75% for BiFab. The molecular weight (Tetra-IgG, ≈240 kDa; Tri-IgG, ≈193 kDa; TriFab, ≈144 kDa; BiFab, ≈100 kDa) and the purity (≥90%) of each construct was confirmed by SDS-PAGE analysis (Figure 1B) and gel filtration (Superdex 200) analysis (Figure S2). QTOF-MS analysis confirmed that all bsAbs were generated through covalent linkage of the desired chain (Table S2).

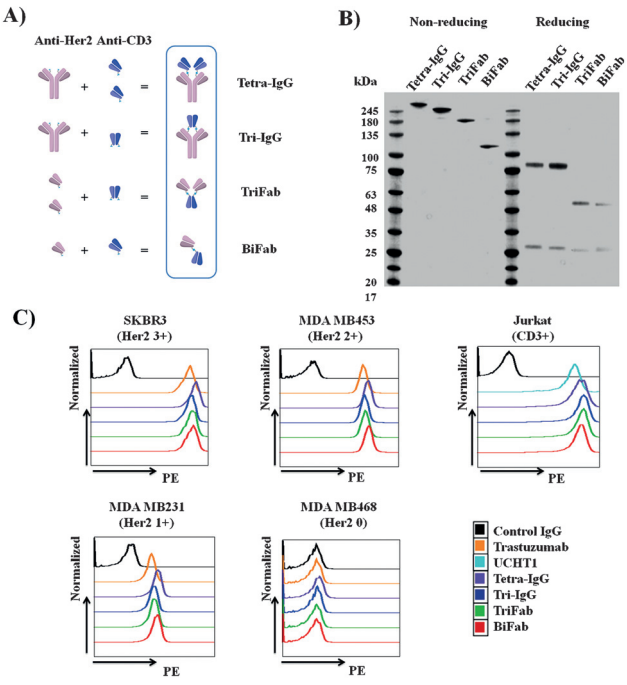

Figure 1. Characterization of anti-Her2/anti-CD3 bsAbs. A) Schematic diagram of bsAb constructs. B) SDS-PAGE analysis of purified bsAbs under nonreducing and reducing conditions. C) Flow cytometry analysis of bsAb constructs and parental antibodies (trastuzumab and UCHT1) binding to different Her2 expressing breast cancer cells and CD3+ Jurkat cells. Cells were consecutively labeled with bsAbs or parental antibodies (25 nM) and secondary PE-conjugated anti-human kappa antibody (eBioscience).

The binding of each bsAb to its antigen was determined by flow cytometry analysis using human T lymphocyte cells (Jurkat, CD3+) and breast cancer cells (SKBR3, Her2 3+; MDA MB453, Her2 2+; MDA MB231, Her2 1+; MDA MB468, Her2 0). The breast cancer cell lines were chosen based on the reported Her2 expression levels that were determined by IHC and FISH,[23–25] and confirmed by flow cytometry analysis (Figure S3). As shown in Figure 1C, all of the conjugates bind both Her2- and CD3-expressing cells to a similar extent (relative binding index of 1810±217 to SKBR3, 673±39 to MDA MB453, 18±2 to MDA MB231, and 598±50 to Jurkat; Table S3), which were comparable to the parental antibodies trastuzumab (relative binding index of 1519 to SKBR3, 626 to MDA MB456, 15 to MDA MB231) and UCHT1 (relative binding index of 410 to Jurkat). More importantly, all the bsAbs failed to bind to the Her2 0 cancer cell, MDA MB468. Overall, these findings highlight an advantageous feature of the semisynthetic approach which largely preserves the binding activity and specificity of parental antibodies after conjugation.

To assess the ability of these bsAbs to selectively direct T cells to Her2 expressing cancer cells, we performed a cytotoxicity assay using different Her2 expressing cancer cells[5,23–29] in the presence of human PBMCs. As shown in Figures 2A and S4, all bsAbs demonstrated excellent cytotoxicity against Her2-expressing cancer cells. A comparison of the half maximal effective concentration (EC_{50}) values indicates that these bsAbs have similar cytotoxicity against the target cells (Table S4). These results demonstrate that different binding valencies to target cells (TriFab versus BiFab) or T cells (Tetra-IgG versus Tri-IgG) do not significantly affect the in vitro potency of bsAbs. This may be attributable to the high affinity of the parental antibodies (trastuzumab $K_d = 0.1$ nM[30] and UCHT1 $K_d = 1.6$ nM[31]), and/or to a similar degree of T-cell activation triggered by TCR

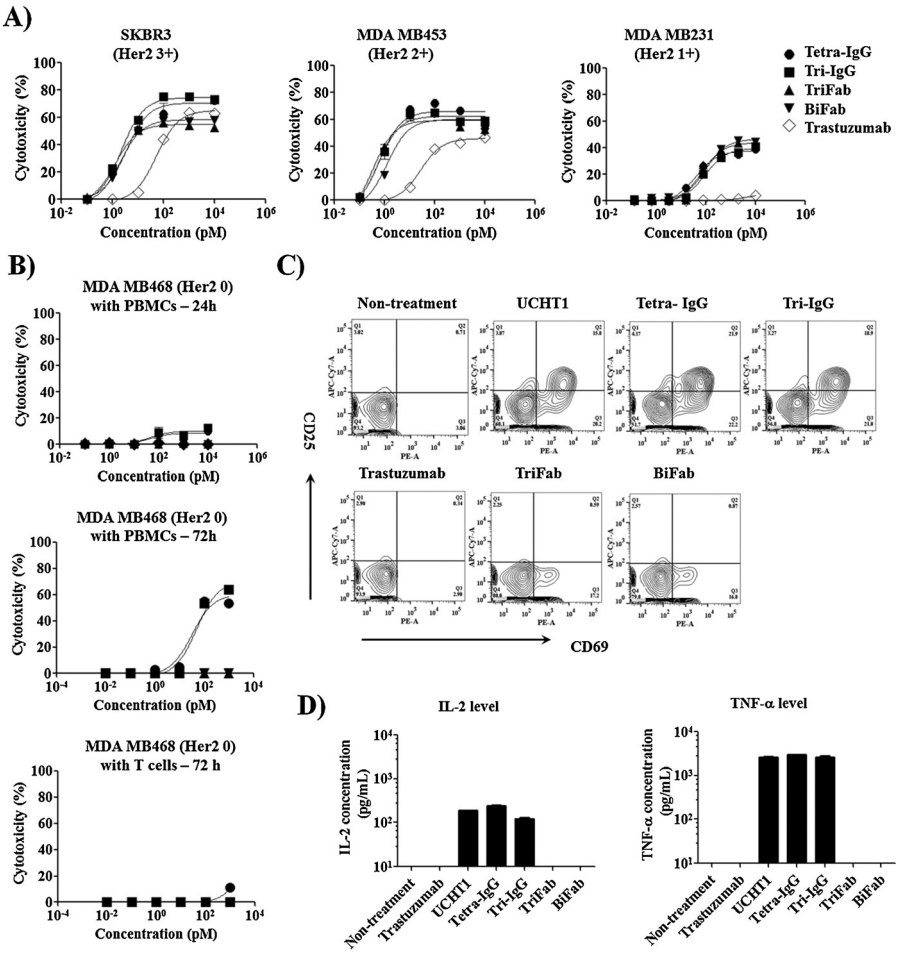

Figure 2. In vitro activity of distinct bsAb formats with different Her2 expressing cancer cells. Effector cells were incubated with target cells at 10:1 ratio for 24 or 72 h. A) 24 h cytotoxic activity of PBMCs against different Her2 expressing cancer cells in the presence of indicated concentrations of bsAbs or trastuzumab. Cytolytic activity was determined by measuring the amount of lactate dehydrogenase (LDH) released into cultured media. B) Comparison of human PBMCs or purified T-cell cytotoxicity induced by IgG- and Fab-based bsAbs against MDA MB468 cells (Her2 0). C) Flow cytometry analysis of T-cell activation markers (CD25 and CD69) in 24 h cultures consisting of MDA MB468, PBMCs, and 100 pM of bsAbs or parental antibodies. D) Quantification of cytokine (IL-2 and TNF-α) levels in the cultures described in (C) by ELISA. Error bars represent standard deviation of duplicate samples.

crosslinking on the cell surface.[32] In addition, in comparison to Her2 3+ and Her2 2+ cells, all bsAbs demonstrated up to 100-fold increase of EC_{50} and an approximate 30% decrease of maximal killing with Her2 1+ cancer cells, which suggest that target cells with higher antigen densities can readily activate T cells with lower concentrations of bsAbs.

Interestingly, at concentrations greater than 100 pM, the IgG-based bsAbs (Tetra-IgG and Tri-IgG) resulted in a higher maximal killing in comparison to the Fab-based constructs (TriFab and BiFab) for Her2 3+ cancer cells (72.7 ± 2.6% versus 56.8 ± 2.4% for SKBR3; 68.3 ± 1.0% versus 48.9 ± 0.5% for HCC1954; 69.4 ± 1.8% versus 53.6 ± 0.8% for MDA MB435/Her2). However, this improved cytolytic effect was not observed when these bsAbs are assayed using cancer cells with reduced Her2 expression (2+ and 1+). This enhanced activity is likely a result of the presence of the Fc domain, which leads to the recruitment of Fc receptor (FcR)-bearing immune cells, as this increase is not observed when purified T cells are used (Figure S5, Table S5). Consistent with this notion, we found that trastuzumab induces Fc-mediated antibody-dependent cellular cytotoxicity (ADCC) with these Her2 overexpressing breast cancer cells (Figures 2A and S4).

We next evaluated if different bsAb formats result in differing degrees of nonspecific T-cell activation which could result in potential off-target toxicity. As shown in Figures 2B and S6, the IgG-based bsAbs (Tetra-IgG and Tri-IgG), but not the Fab-based bsAbs, induced antigen-independent cytotoxic activity against Her2 0 breast cancer cells (MDA MB468) in the presence of PBMCs after 24 h. This nonspecific cytotoxicity was more evident in an extended (72 h) culture with PBMCs, but was not observed with purified T cells (Figure 2B). In addition, as shown in Figure 2C, 24 h cultures treated with the IgG-based bsAbs resulted in an upregulation of T-cell activation markers (CD25 and CD69) to a similar degree as full-length UCHT1, whereas both trastuzumab and the Fab-based constructs did not activate T cells. Likewise, Tetra-IgG, Tri-IgG, and UCHT1 enhanced inflammatory cytokine (IL2 and TNF-α) secretion and granzyme B expression (Figures 2D and S7). To further confirm whether the Fc-FcR interaction is responsible for the observed nonspecific activation of T cells, we generated an Fc null version of Tetra-IgG, in which two residues (L237 and L238) in the Fc domain were mutated to alanine to minimize FcR-binding.[33] Similar to BiFab, Tetra-IgG (Fc null) showed reduced nonspecific killing of MDA MB468 cells in comparison to Tetra-IgG (Fc intact; Figure S8). Overall, our findings demonstrate that bsAb constructs containing the CD3 binding domain and a functional Fc domain can specifically crosslink T cells with FcR-positive immune cells, resulting in the activation of T cells in an antigen-independent manner. This observation is consistent with previous preclinical reports,[34,35] including safety data from a clinical trial with ertumaxomab, an IgG-version bsAb with a functional Fc domain, in which nearly all the patients developed symptoms of CRS.[36] Nonetheless, the reduced nonspecific activity of Tetra-IgG (Fc null) suggests that a mutational approach can potentially improve the safety of IgG-like bsAbs.

We next compared the efficacy of bsAbs with a previously reported Her2-targeted ADC, T-nAF, in which the cytotoxic drug monomethyl auristatin is site-specifically conjugated to a mutant trastuzumab bearing pAcF at the heavy chain residue of A121 (35). This homogeneous T-nAF (with a drug to antibody ratio of two) was reported to have excellent in vitro and in vivo efficacies (eradicates Her2 3+ tumors in a SCID mouse xenograft model with a single dose of T-nAF at 5 mg kg^{-1}).[20,37,38] In 24 h cytotoxicity assays using PBMCs, T-nAF elicited appreciable but lower activity compared to the bsAbs against Her2 3+ and 2+ cells (Figures 3A and S9, and Table S6); this difference in cytotoxicity increased further after 72 h (Figure S10 and Table S7). Of particular note, T-nAF failed to lyse Her2 1+ cancer cells in 24 h and 72 h cultures, which is consistent with preclinical data reported for T-DM1.[5] In contrast, bsAb treatment resulted in efficient lysis of Her2 1+ cancer cells. In order for an ADC such as T-nAF to have efficacy, the antibody/antigen complex must be internalized and the drug is released within the target cell.[39] Accordingly, we assessed the internalization of T-nAF by immunofluorescent staining, and observed that T-nAF is present in Her2 3+ and 2+ cells, but not in Her2 1+ and 0 cells (Figure 3B). However, as shown in Figure 3C, we observed efficient recruitment of T cells (green) to the target cells (red) in the presence of bsAbs (Tetra-IgG or BiFab) in all Her2 expressing cancer cells (Her2 3+, 2+, and 1+), but not Her2 0 cells, supporting the increased antigen sensitivity of bsAbs over T-nAF that was observed in the cytotoxicity assays.

To determine whether the activity observed in in vitro assays translates to in vivo mouse xenograft models, we first evaluated the pharmacokinetics of bsAbs by i.v. injection into CD1 female mice. The IgG-based bsAbs (Tetra-IgG and Tri-IgG) have similar elimination half-lives of 79.9 ± 1.6 h and 79.5 ± 0.5 h, respectively. On the other hand, the Fab-based bsAbs, TriFab and BiFab, were cleared more rapidly from circulation, with elimination half-lives of 4.4 ± 0.3 h and 3.0 ± 0.2 h, respectively (Figure S11). This rapid clearance of the Fab-based bsAbs may require more frequent dosing in humans, but may offer improved ability to control the T-cell response. To evaluate the in vivo efficacy of selected bsAbs (Tetra-IgG and BiFab) and compare them with T-nAF, xenograft models were established by subcutaneous implantation of Her2 3+ (HCC1954) or Her2 2+ (MDA MB453) cells in female NSG mice. Upon the formation of a palpable tumor, mice were infused with human T cells into the peritoneal cavity. On the basis of the different half-lives and molecular weights of each molecule, mice were intravenously administered T-nAF (147 kDa, 5 mg kg^{-1}, one dose), Tetra-IgG (240 kDa, 10 mg kg^{-1}, one dose), BiFab (100 kDa, 1 mg kg^{-1}, seven doses every other day), or saline and observed for 5 weeks. As shown in Figure 4A and B, mice treated with either T-nAF or bsAbs (Tetra-IgG or BiFab) demonstrated significant inhibition of tumor growth in both the Her2 3+ and Her2 2+ groups in comparison to the control group in which mice only received T cells and saline. Infusion of T cells together with T-nAF did not affect the complete regression of established Her2 3+ and 2+ tumors, confirming our previous results.[20,37] Next, we evaluated the same agents in Her2 1+ (MDA MB231 and MDA MB435) xenograft models. In these studies, the dosing regimen for T-nAF and bsAbs was the same as that described above. In consideration of the limited number and potentially

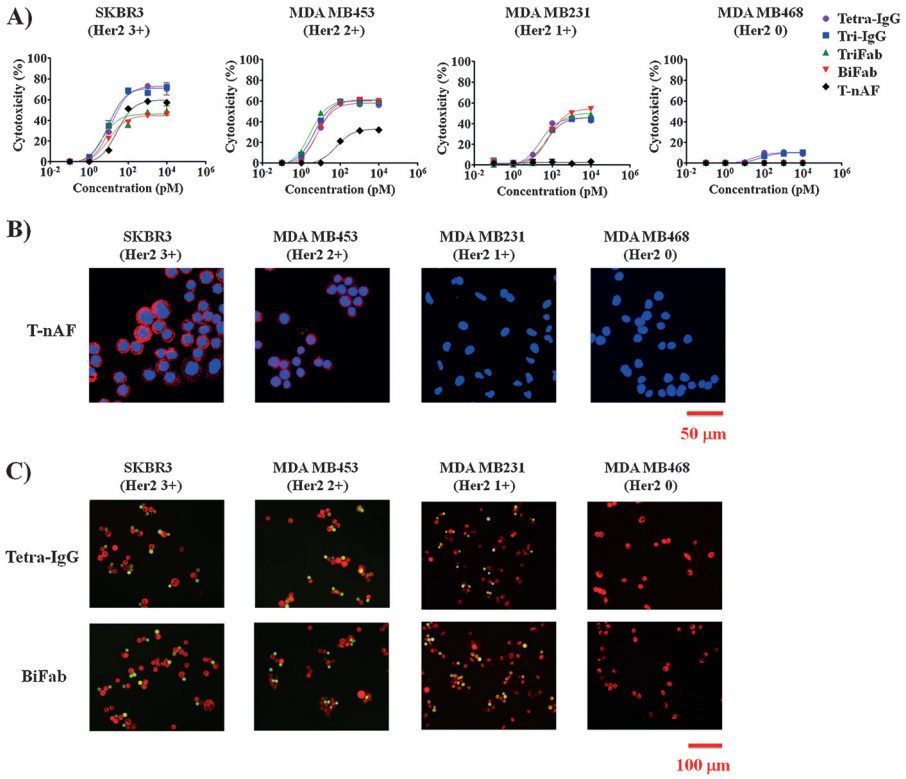

Figure 3. In vitro characterization of T-nAF and bsAbs with different Her2 expressing breast cancer cells. A) 24 h cytotoxicity assays were performed with human PBMCs and indicated target cells at 10:1 ratio in the presence of different concentrations of T-nAF or bsAbs. Error bars represent standard deviation of duplicate samples. B) Internalization analysis on breast cancer cells after 4 h treatment with 20 nM T-nAF. After the removal of surface-bound T-nAF by an acid wash, internalized T-nAF was detected with Alexa fluor 555-labeled anti-human IgG (red), and imaged by confocal microscopy (Zeiss 710). Hoechst 33342 (blue) was used for nuclear counterstaining. C) Analysis of the crosslinking of cancer cells and T cells. Fluorescently labeled target cells (red) and T cells (green) were mixed at a 1:1 ratio, and incubated for 4 h in the presence of 20 nM Tetra-IgG or BiFab. Nonconjugated cells were gently removed by PBS wash for three times, prior to imaging on a fluorescence microscope (Nikon Eclipse).

short lifespan of adoptively transferred human T cells in the mice, we infused T cells multiple times during the treatment (three infusions with six days between each time). As shown in Figure 4C and D, mice treated with Tetra-IgG and BiFab showed significant tumor growth delay in comparison to the control group ($p < 0.005$ for MDA MB231 and $p < 0.05$ for MDA MB435), whereas T-nAF was marginally effective in both Her2 1+ xenograft models ($p > 0.1$). In tissue distribution studies with tumor-bearing (MDA MB435/Her2) NSG mice, both bsAbs demonstrated good tumor localization. Consistent with a longer half-life, Tetra-IgG demonstrated a nine-fold higher radiant efficiency compared to BiFab at 72 h after i.v. injection ($47.2 \pm 8.6 \times 10^8$ versus $5.3 \pm 2.1 \times 10^8$ (photons/s/cm^2/steradian)/(μW/cm^2), respectively) (Figures S12 and S13). The tumor-to-muscle ratio (TMR) of bsAbs in organs and tissues dissected at 72 h post injection is summarized in Figure S14, showing that Tetra-IgG accumulation in the tumor is higher than BiFab.

Overall, the in vivo efficacy studies verified our in vitro findings and further support the notion that bsAbs are highly effective for targeting breast cancer cells with antigens of low abundance. Further comprehensive in vivo studies, including dose titration studies, are necessary to determine the optimal dosage of bsAbs. Moreover, future surrogate studies in immunocompetent mice will provide additional information regarding the efficacy and safety of bsAbs. In conclusion, the data presented here suggest that the monovalent BiFab in the absence of an Fc domain may be the best bsAb format to trigger antigen-dependent T-cell activation and target tumor eradication for low or heterogeneous Her2 expressing cancers.

Keywords: antibody drug conjugates · T-cell activation · bispecific antibodies · breast cancers · noncanonical amino acids

How to cite: *Angew. Chem. Int. Ed.* **2015**, *54*, 7022–7027
Angew. Chem. **2015**, *127*, 7128–7133

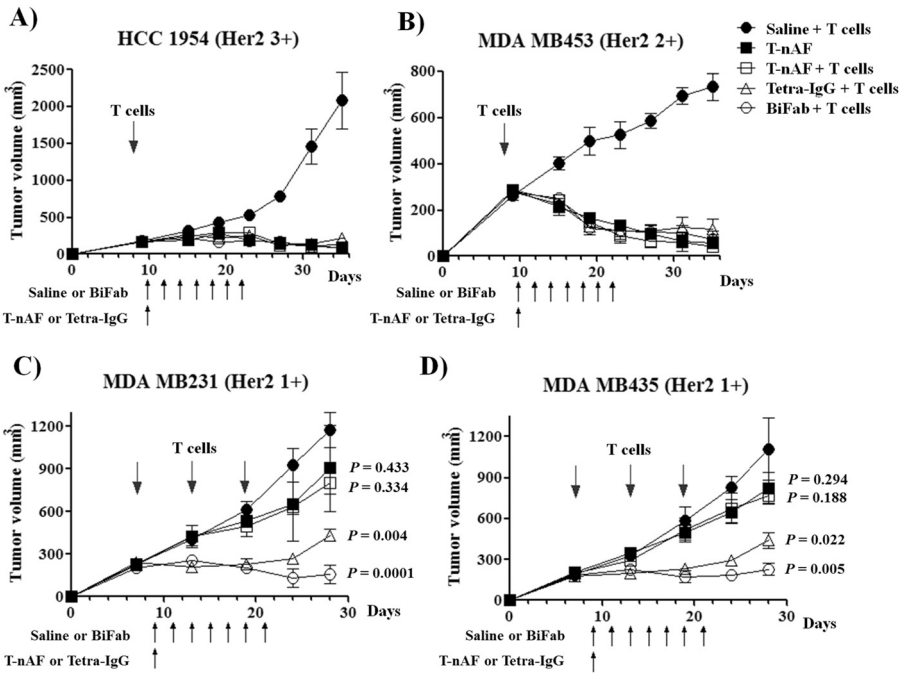

Figure 4. In vivo efficacy comparison of T-nAF and bsAbs in human breast cancer xenograft models. For HCC1954 (A) and MDA MB453 (B) xenograft studies, eight days after subcutaneous implantation of 5×10^6 cancer cells in 50% Matrigel, female NSG mice received one intraperitoneal (IP) injection of 30×10^6 activated T cells. For MDA MB231 (C) and MDA MB435 (D) xenograft studies, seven days after subcutaneous implantation of 20×10^6 or 2×10^6 cancer cells in 50% Matrigel, respectively, mice were injected three times with 20×10^6 activated T cells every six days via IP. For all studies, two days after the initial T-cell infusion, mice were treated intravenously with one dose of T-nAF (5 mg kg^{-1}) or Tetra-IgG (10 mg kg^{-1}), or seven doses of BiFab (1 mg kg^{-1}) or saline every other day. Tumors were measured twice a week with calipers, and tumor volume was calculated by W × L × H. Each data point represent mean tumor volume of five mice in each group ± SD. Arrows indicate the time of activated PBMC injections or of treatment with specified therapeutics. *P* values < 0.05 compared to the control groups (saline + T cells) were considered significant.

[1] C. L. Vogel, M. A. Cobleigh, D. Tripathy, J. C. Gutheil, L. N. Harris, L. Fehrenbacher, D. J. Slamon, M. Murphy, W. F. Novotny, M. Burchmore, S. Shak, S. J. Stewart, M. Press, *J. Clin. Oncol.* **2002**, *20*, 719–726.
[2] I. Krop, E. P. Winer, *Clin. Cancer Res.* **2014**, *20*, 15–20.
[3] G. M. Keating, *Drugs* **2012**, *72*, 353–360.
[4] M. A. Owens, B. C. Horten, M. M. Da Silva, *Clin. Breast Cancer* **2004**, *5*, 63–69.
[5] G. D. Lewis Phillips, G. Li, D. L. Dugger, L. M. Crocker, K. L. Parsons, E. Mai, W. A. Blattler, J. M. Lambert, R. V. Chari, R. J. Lutz, W. L. Wong, F. S. Jacobson, H. Koeppen, R. H. Schwall, S. R. Kenkare-Mitra, S. D. Spencer, M. X. Sliwkowski, *Cancer Res.* **2008**, *68*, 9280–9290.
[6] D. Müller, R. E. Kontermann, *BioDrugs* **2010**, *24*, 89–98.
[7] L. Ducry, B. Stump, *Bioconjugate Chem.* **2010**, *21*, 5–13.
[8] M. Jager, A. Schoberth, P. Ruf, J. Hess, H. Lindhofer, *Cancer Res.* **2009**, *69*, 4270–4276.
[9] T. T. Junttila, J. Li, J. Johnston, M. Hristopoulos, R. Clark, D. Ellerman, B. E. Wang, Y. Li, M. Mathieu, G. Li, J. Young, E. Luis, P. G. Lewis, E. Stefanich, C. Spiess, A. Polson, B. Irving, J. M. Scheer, M. R. Junttila, M. S. Dennis, R. Kelley, K. Totpal, A. Ebens, *Cancer Res.* **2014**, *74*, 5561–5571.
[10] R. Lutterbuese, T. Raum, R. Kischel, P. Hoffmann, S. Mangold, B. Rattel, M. Friedrich, O. Thomas, G. Lorenczewski, D. Rau, E. Schaller, I. Herrmann, A. Wolf, T. Urbig, P. A. Baeuerle, P. Kufer, *Proc. Natl. Acad. Sci. USA* **2010**, *107*, 12605–12610.
[11] M. Cioffi, J. Dorado, P. A. Baeuerle, C. Heeschen, *Clin. Cancer Res.* **2012**, *18*, 465–474.
[12] Y. Gao, D. Xiong, M. Yang, H. Liu, H. Peng, X. Shao, Y. Xu, C. Xu, D. Fan, L. Qin, C. Yang, Z. Zhu, *Leukemia* **2004**, *18*, 513–520.

[13] S. L. Maude, D. Barrett, D. T. Teachey, S. A. Grupp, *Cancer J.* **2014**, *20*, 119 – 122.
[14] P. Fournier, V. Schirrmacher, *BioDrugs* **2013**, *27*, 35 – 53.
[15] P. Chames, D. Baty, *MAbs* **2009**, *1*, 539 – 547.
[16] C. H. Kim, J. Y. Axup, A. Dubrovska, S. A. Kazane, B. A. Hutchins, E. D. Wold, V. V. Smider, P. G. Schultz, *J. Am. Chem. Soc.* **2012**, *134*, 9918 – 9921.
[17] W. Liu, A. Brock, S. Chen, S. Chen, P. G. Schultz, *Nat. Methods* **2007**, *4*, 239 – 244.
[18] L. Wang, A. Brock, B. Herberich, P. G. Schultz, *Science* **2001**, *292*, 498 – 500.
[19] B. M. Hutchins, S. A. Kazane, K. Staflin, J. S. Forsyth, B. Felding-Habermann, P. G. Schultz, V. V. Smider, *J. Mol. Biol.* **2011**, *406*, 595 – 603.
[20] J. Y. Axup, K. M. Bajjuri, M. Ritland, B. M. Hutchins, C. H. Kim, S. A. Kazane, R. Halder, J. S. Forsyth, A. F. Santidrian, K. Stafin, Y. Lu, H. Tran, A. J. Seller, S. L. Biroc, A. Szydlik, J. K. Pinkstaff, F. Tian, S. C. Sinha, B. Felding-Habermann, V. V. Smider, P. G. Schultz, *Proc. Natl. Acad. Sci. USA* **2012**, *109*, 16101 – 16106.
[21] J. Dommerholt, S. Schmidt, R. Temming, L. J. Hendriks, F. P. Rutjes, J. C. van Hest, D. J. Lefeber, P. Friedl, F. L. van Delft, *Angew. Chem. Int. Ed.* **2010**, *49*, 9422 – 9425; *Angew. Chem.* **2010**, *122*, 9612 – 9615.
[22] J. E. Hudak, R. M. Barfield, G. W. de Hart, P. Grob, E. Nogales, C. R. Bertozzi, D. Rabuka, *Angew. Chem. Int. Ed.* **2012**, *51*, 4161 – 4165; *Angew. Chem.* **2012**, *124*, 4237 – 4241.
[23] D. M. Collins, N. O'Donovan, P. M. McGowan, F. O'Sullivan, M. J. Duffy, J. Crown, *Ann. Oncol.* **2012**, *23*, 1788 – 1795.
[24] K. McLarty, B. Cornelissen, D. A. Scollard, S. J. Done, K. Chun, R. M. Reilly, *Eur. J. Nucl. Med. Mol. Imaging* **2009**, *36*, 81 – 93.
[25] J. W. Park, K. Hong, D. B. Kirpotin, G. Colbern, R. Shalaby, J. Baselga, Y. Shao, U. B. Nielsen, J. D. Marks, D. Moore, D. Papahadjopoulos, C. C. Benz, *Clin. Cancer Res.* **2002**, *8*, 1172 – 1181.
[26] L. DeFazio-Eli, K. Strommen, T. Dao-Pick, G. Parry, L. Goodman, J. Winslow, *Breast Cancer Res.* **2011**, *13*, R44.
[27] J. L. Nordstrom, S. Gorlatov, W. Zhang, Y. Yang, L. Huang, S. Burke, H. Li, V. Ciccarone, T. Zhang, J. Stavenhagen, S. Koenig, S. J. Stewart, P. A. Moore, S. Johnson, E. Bonvini, *Breast Cancer Res.* **2011**, *13*, R123.
[28] L. D. Tan, Y. Y. Xu, Y. Yu, X. Q. Li, Y. Chen, Y. M. Feng, *PLoS One* **2011**, *6*, e18764.
[29] I. O. Ellis, J. Bartlett, M. Dowsett, S. Humphreys, B. Jasani, K. Miller, S. E. Pinder, A. Rhodes, R. Walker, *J. Clin. Pathol.* **2004**, *57*, 233 – 237.
[30] J. Baselga, *Ann. Oncol.* **2001**, *12 Suppl 1*, S49-S55.
[31] D. A. Cantrell, A. A. Davies, M. J. Crumpton, *Proc. Natl. Acad. Sci. USA* **1985**, *82*, 8158 – 8162.
[32] D. A. Schmid, M. B. Irving, V. Posevitz, M. Hebeisen, A. Posevitz-Fejfar, J. C. Sarria, R. Gomez-Eerland, M. Thome, T. N. Schumacher, P. Romero, D. E. Speiser, V. Zoete, O. Michielin, N. Rufer, *J. Immunol.* **2010**, *184*, 4936 – 4946.
[33] K. C. Herold, S. E. Gitelman, U. Masharani, W. Hagopian, B. Bisikirska, D. Donaldson, K. Rother, B. Diamond, D. M. Harlan, J. A. Bluestone, *Diabetes* **2005**, *54*, 1763 – 1769.
[34] B. K. Link, S. A. Kostelny, M. S. Cole, W. P. Fusselman, J. Y. Tso, G. J. Weiner, *Int. J. Cancer* **1998**, *77*, 251 – 256.
[35] R. Belani, G. J. Weiner, *J. Hematother.* **1995**, *4*, 395 – 402.
[36] P. Kiewe, S. Hasmuller, S. Kahlert, M. Heinrigs, B. Rack, A. Marme, A. Korfel, M. Jager, H. Lindhofer, H. Sommer, E. Thiel, M. Untch, *Clin. Cancer Res.* **2006**, *12*, 3085 – 3091.
[37] F. Tian, Y. Lu, A. Manibusan, A. Sellers, H. Tran, Y. Sun, T. Phuong, R. Barnett, B. Hehli, F. Song, M. J. DeGuzman, S. Ensari, J. K. Pinkstaff, L. M. Sullivan, S. L. Biroc, H. Cho, P. G. Schultz, J. DiJoseph, M. Dougher, D. Ma, R. Dushin, M. Leal, L. Tchistiakova, E. Feyfant, H. P. Gerber, P. Sapra, *Proc. Natl. Acad. Sci. USA* **2014**, *111*, 1766 – 1771.
[38] D. Jackson, J. Atkinson, C. I. Guevara, C. Zhang, V. Kery, S. J. Moon, C. Virata, P. Yang, C. Lowe, J. Pinkstaff, H. Cho, N. Knudsen, A. Manibusan, F. Tian, Y. Sun, Y. Lu, A. Sellers, X. C. Jia, I. Joseph, B. Anand, K. Morrison, D. S. Pereira, D. Stover, *PLoS One* **2014**, *9*, e83865.
[39] Y. Cao, J. W. Marks, Z. Liu, L. H. Cheung, W. N. Hittelman, M. G. Rosenblum, *Oncogene* **2014**, *33*, 429 – 439.

Received: January 27, 2015
Revised: March 16, 2015
Published online: April 27, 2015

